Diffuse Microstructural Abnormalitites in Non-Cystic Focal White Matter Necrosis

A. C. Nagasunder[1], L. Paquette[2], C. J. Tavare[3], T. Rosser[4], F. H. Gilles[3], M. D. Nelson[1], S. Bluml[1,5], and A. Panigrahy[1,6]

[1]Department of Radiology, Childrens Hospital Los Angeles, Los Angeles, California, United States, [2]Division of Neonatology, Childrens Hospital Los Angeles, Los Angeles, California, United States, [3]Department of Neuropathology, Childrens Hospital Los Angeles, Los Angeles, California, United States, [4]Division of Neurology, Childrens Hospital Los Angeles, Los Angeles, California, United States, [5]Rudi Schulte Research Institute, Santa Barbara, California, United States, [6]Department of Radiology, Childrens Hospital of Pittsburgh of UPMC, Pittsburgh, Pennsylvania, United States

Purpose: To determine if there are diffuse microstructural abnormalities associated with non-cystic focal white matter necrosis (periventricular leukomalacia PVL) in a diverse cohort of neonates scanned at term equivalent age.

Methods: Diffusion Tensor data were retrospectively reviewed in this IRB approved study. Eighteen patients with T1-hyperintensity SPGR focal lesions and twenty term controls were included. DTI protocol consisted of echo planar imaging (EPI) sequence using neonatal head coil with 25 directions and b=700s/mm^2 on a 1.5T GE Scanner. Grey matter (GM) structures and white matter (WM) structures were manually traced **(Fig.1)** on maps generated by DTIStudio (John Hopkins, MD, USA). Clinical correlative data including gestational age, sepsis and congenital heart disease was collected. Statistical comparison was performed using ANOVA with Bonferroni correction for multiple comparisons.

Results: On radiological examination, focal necroses were predominantly located bilaterally in frontal WM, optic radiation and centrum semiovale **(Fig.2A)**. 40% cases were premature, 60% term and 56% had congential heart disease. DTI analyses showed anisotropy of splenium to be significantly decreased in focal PVL cases **(Table)**. Radial diffusivity of splenium, frontal WM and anterior frontal WM were significantly increased compared to controls. Decreased anisotropy of genu, splenium and increased radial diffusivity of the splenium, sensorimotor region correlated with extent of necrosis. (p<0.008) **(Fig.3)**

Discussion: This study shows microstructural abnormalities in regions of the brain separate from the focal necroses. Reduced fractional anisotropy and increased radial diffusivity have been associated with demyelination in long tracts in animal models, suggesting that the microstructural changes in the splenium may be secondary to diffuse white matter injury in the parietal regions. Likewise, these results in unmyelinated tissue have been associated with pre-oligodendrocyte injury. Diffuse injury in periperal white matter is more likely related to disrupted premyelinating oligodendroglia compared to disrupted axons in which a predominated axial diffusivity abnormality would be detected. High incidence of focal necrosis was found in term infants. There were no specific microstructural abnormalities of the grey matter structures.

Conclusion: DTI can be used to detect diffuse microstructural injury in white matter regions both proximal and distant from necrotic foci (PVL).

Acknowledgements: Grant support: Rudi Schulte Research Institute, NIH NS 063371, CHLA GCRC grant CCI-06-00121

References: 1. Haynes et al. Pediatr Res 63(6):656-661, 2008. 2. Cheong et al. AJNR 2009. 3. Amanda et al. Pediatr Res, 2009

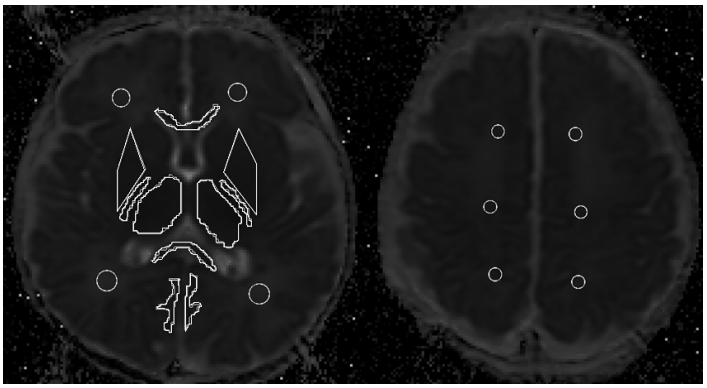

Fig.1: *Manually traced regions of interest at two different levels on apparent diffusion coefficient map (ADC).*

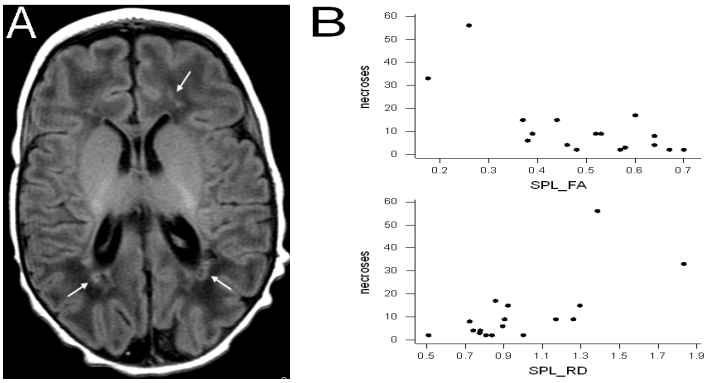

Fig.2A: *Focal necroses in frontal WM and optic radiation (arrows).* ***2B:*** *Correlation between extent of necrosis and fractional anisotropy (FA) and radial diffusivity (RD) of the splenium (SPL).*

Table: DTI metrics of structures

		Control n=20 mean (SD)	Focal PVL n=18 mean (SD)	p
PCA (weeks)		45.13 (3.19)	43.93 (6.69)	.478
Splenium	FA	.59 (.08)	.49 (.14)	.012
	RA	.57 (.10)	.46 (.16)	.013
	AD	2.19 (.34)	2.25 (.38)	.574
	RD	.76 (.20)	.98 (.32)	.014
	MD	1.24 (.22)	1.41 (.27)	.049
Frontal WM *	FA	.19 (.07)	.14 (.06)	.034
	RA	.16 (.06)	12 (.05)	.041
	AD	1.70 (.25)	1.91 (.41)	.059
	RD	1.29 (.29)	1.56 (.40)	.021
	MD	1.43 (.27)	1.69 (.39)	.023
Parietal WM *	FA	.19 (.05)	.18 (.05)	.377
	RA	.16 (.05)	.15 (.04)	.365
	AD	1.77 (.34)	1.88 (.37)	.319
	RD	1.33 (.28)	1.47 (.33)	.186
	MD	1.48 (.29)	1.62 (.33)	.180
Anterior WM *	FA	.24 (.04)	.20 (.07)	.038
	RA	.20 (.04)	.17 (.06)	.048
	AD	1.63 (.23)	1.85 (.34)	.023
	RD	1.16 (.19)	1.39 (.32)	.009
	MD	1.32 (.20)	1.55 (.32)	.011

* Bilateral regions were averaged to get single value
RA=relative anisotropy, AD=axial diffusivity, MD=mean diffusivity